





## ARTICLE

## Spatiotemporal Hotspots of Juvenile Bigeye and Yellowfin Tuna Catches Under Drifting Fish-Aggregating Devices in the Eastern Atlantic Ocean to Define Moratorium Strata

Sosthene Alban Valeryn Akia<sup>1,2,3</sup> 🕞 | Loreleï Guéry<sup>4,5</sup> | Pedro J. Pascual-Alayón<sup>6</sup> | Daniel Gaertner<sup>1,2</sup>

<sup>1</sup>MARBEC, IRD, Univ Montpellier, CNRS, Ifremer, Sète, France | <sup>2</sup>Institut de Recherche Pour le Développement (IRD), UMR MARBEC, Sète Cedex, France | <sup>3</sup>Fisheries and Oceans Canada (DFO), Saint Andrews Biological Station, Nouveau Brunswick, Canada | <sup>4</sup>CIRAD, UMR PHIM, Montpellier, France | <sup>5</sup>CIRAD, INRAE, Institut Agro, IRD, PHIM, University of Montpellier, Montpellier, France | <sup>6</sup>Instituto Español de Oceanografía, Centro Oceanográfico de Canarias, Santa Cruz de Tenerife, Spain

Correspondence: Sosthene Alban Valeryn Akia (sosthene.akia@dfo-mpo.gc.ca)

Received: 21 June 2024 | Revised: 21 October 2024 | Accepted: 23 October 2024

**Funding:** This research was co-funded by the French Directorate general for Maritime affairs, Fisheries and Aquaculture (DGAMPA) and the "Observatoire des Ecosystèmes Pélagiques Tropicaux exploités" (Ob7) from IRD/MARBEC.

Keywords: dFAD hotspots | Eastern Atlantic Ocean | emerging hotspot analysis | juvenile tropical tuna | time-area closure | VAST method

#### **ABSTRACT**

To reduce catches of juvenile bigeye and yellowfin tuna, while maintaining skipjack catches under drifting fish aggregating devices (dFAD), we analyzed spatiotemporal distributions of dFAD catches by European purse seiners in the Eastern Atlantic Ocean during 1996–2019. To detect hotspots of juvenile dFAD catches, we: identified periods of maximum abundance using a seasonal sub-series diagram; normalized monthly FAD catches per unit effort; and used emerging hotspots analysis on spatiotemporal density. Two main spatiotemporal strata were identified in the Guinean Gulf, which could be used to establish moratoria on dFAD fishing. These spatiotemporal strata differed from the existing ICCAT moratorium, which spanned a larger part of the African coast. Our findings also indicated that time-area closures of dFAD-fishing lasting 3–4 months in smaller areas could be more effective than the current dFAD moratorium to reduce unwanted bycatch in the Eastern Atlantic region. The two metrics we developed for comparison provided clear and measurable evidence that demonstrated how strategic and data-informed moratoriums can lead to substantial improvements in conservation.

## 1 | Introduction

Tropical tunas, particularly bigeye (*Thunnus obesus*, BET), yellowfin (*Thunnus albacares*, YFT), and skipjack (*Katsuwonus pelamis*, SKJ), play crucial roles in global marine ecosystems and are economically important for many nations (FAO 2020). These species are the primary targets of large-scale industrial fisheries, especially in tropical and subtropical waters across the Atlantic, Indian, and Pacific oceans (Rogers et al. 2016). The purse seine fishery, which encircles schools of tuna with large nets, is one of the most efficient methods for capturing these species, especially in the Atlantic Ocean (Miyake et al. 2010). Purse-seine

vessels account for about 66% of the 5.2 million tons of tuna caught annually worldwide (ISSF 2024). A vertical net 'curtain' is used to surround a school of fish, the bottom of which is then drawn together to enclose the fish, like tightening the cords of a drawstring purse (https://www.msc.org/what-we-are-doing/our-approach/fishing-methods-and-gear-types/purse-seine).

However, increasing pressure on tuna stocks has raised concerns about their sustainability. Recent stock assessments of Atlantic tropical tunas by ICCAT indicated varying levels of concern. The skipjack tuna stock is generally considered to be in good health, with the latest assessments suggesting it is

© 2024 John Wiley & Sons Ltd.

neither overfished nor subject to overfishing (ICCAT 2022). Yellowfin tuna is also not overfished and not subject to overfishing (ICCAT 2019). In contrast, the assessment results show that in 2021, the Atlantic bigeye tuna stock was overfished, with the stock below the biomass level that can produce maximum sustainable yield and was not overfished at that time (ICCAT 2021).

Following the increasing use of drifting Fishing Aggregating Devices (dFAD) in the early 1990s, tuna Regional fisheries management organizations (RFMOs) were quickly confronted with the trade-off between reducing mortality on juvenile bigeye and yellowfin tuna, but without significantly reducing skipjack catches, because skipjack is the predominant species in dFAD catches (Ariz et al. 1999; Hallier and Parajúa 1999). Among the many measures included in tuna fisheries management, timearea closures of FAD-fishing for mitigating juvenile bycatch have become more important over the last decades. Following a voluntary moratorium observed by European purse seiners in 1997-1998 (Goujon 1998), several moratoria on dFAD were implemented since 1999 in the Atlantic Ocean by the International Commission for the Conservation of Atlantic Tunas (ICCAT). However, different choices of periods and areas of closure of the dFAD fishery were not based on ecological or scientific knowledge resulting from proposals made by the Standing Committee on Research and Statistics (SCRS) of ICCAT, so the effectiveness of different dFAD moratoria was questioned (Fonteneau et al. 2016).

With this consideration in mind, mapping dFAD hotspots of juvenile tunas, or vulnerable associated pelagic species, may give spatially explicit solutions for effective area-based management, with the aim of contributing to the sustainability of the tropical tuna fishery as part of an ecosystem approach to fisheries management (Garcia and Cochrane 2005). Hotspots can be located based on catches, catch per unit effort (CPUE), or the ratio of catch of a species to be protected to a target species (Harley and Suter 2007). In the case of a multi-species fishery like the tropical tuna seine fishery, the use of self-organizing maps showing catch hotspots can be used as a visual aid by decision-makers to identify candidate areas for seasonal and spatial closure (Stephan et al. 2022). However, to be effective in reducing the mortality of juvenile tuna, time-area closures should be placed in strata where (1) monthly catches are historically high and (2) hotspots are predictable in time and space.

We aimed to identify dFAD catch hotspots for small tropical tunas in the eastern Atlantic Ocean and to track their evolution over a 24-year period (1996-2019), with the end goal of recommending optimal moratorium zones. To achieve this objective, we examined seasonality of monthly catches and fishing effort to identify peak months for small tropical tuna catches. We applied the VAST (Vector Autoregressive Spatiotemporal) method, a specific geostatistical generalized linear mixed model (GLMM) to standardize catch per unit effort for each species. This allowed us to forecast local monthly biomass density throughout the fishing domain frequented by French and Spanish purse seiners in the Eastern Atlantic. The VAST approach adjusted for factors that impact catch per unit effort to minimize biases by accounting for the influence of past moratoria and other elements that affect catchability of tuna. Local biomass density extracted from VAST were used in an emerging hotspot analysis

(EHSA) to determine monthly hotspot zones and evaluate fluctuations of hotspots during the study period. A final step used spatial maps generated from the hotspot analysis to gauge overlap among species. We hoped our findings would inform decisions about balancing the reduction of juvenile bigeye and yellowfin tuna catches against maintenance of skipjack catches, and subsequently guide recommendations for new, more suitable spatiotemporal strata for dFAD moratoria.

## 2 | Materials and Methods

#### 2.1 | Data Sources

Data were sourced from logbooks of European tropical tuna purse-seiners (France and Spain), the largest surface fishing fleet in the eastern Atlantic (48% of all tropical purse-seine catch during 1996-2019). Operational fishing grounds for these purse seiners extended between latitudes 20°S and 20°N and longitudes 35° W and 15° E and were representative of all purseseine fleets, some of which belonged to European companies (Figure 1). Catch and effort data were compiled and managed by the Tuna Observatory (Ob7) of the French National Research Institute for Sustainable Development (IRD, UMR MARBEC) for the French fleet and by the Spanish Institute of Oceanography (IEO) for the Spanish fleet. Each record of a fishing set contained information on the date, geographical location, school type, estimated catch, and composition of tuna species in size categories: 0-10, 10-30, and  $\geq$  30 kg. The T3 methodology corrected raw logbook data produced by skippers for total catch per set and species composition (based on port size and species sampling, Pallarés and Hallier 1997; Duparc et al. 2020). These processed data were the "level 1" logbook database used in this study. Commercial size categories were used to distinguish stages of tropical tuna: < 10 kg were mainly skipjack, with some juvenile yellowfin and bigeye, and classified as category 1; and ≥10 kg were mainly yellowfin and bigeye, and classified as categories 2 and 3 (Escalle et al. 2016). Due to the study objective, we used only data for commercial category 1 caught by European purse seiners. Catch and effort statistics for each species were collected in small areas (1×1° squares for most gears, and 5×5° squares for longlines), gear, flag, and month, identified as ICCAT Task 2 data.

## 2.2 | Seasonal Subseries Plots

Seasonal subseries plots (Cleveland 1993), also known as seasonal plots, were used to analyze and visualize seasonal patterns in multi-year time-series data. By organizing data into inherent seasonal periods (like months or quarters), plots highlighted seasonal components with the response variable on the vertical axis and time organized by season on the horizontal axis. A reference line at the group means identified annual recurring patterns to assess seasonality, within-group patterns, and outliers.

For the 24-year dataset, seasonal subseries plots used: (1) raw monthly catch values and (2) the percentage of monthly catches relative to their respective years. To discern variation in seasonal patterns over shorter periods, the 24-year period was divided into four 6-year subperiods for raw monthly catch analysis. Seasonal

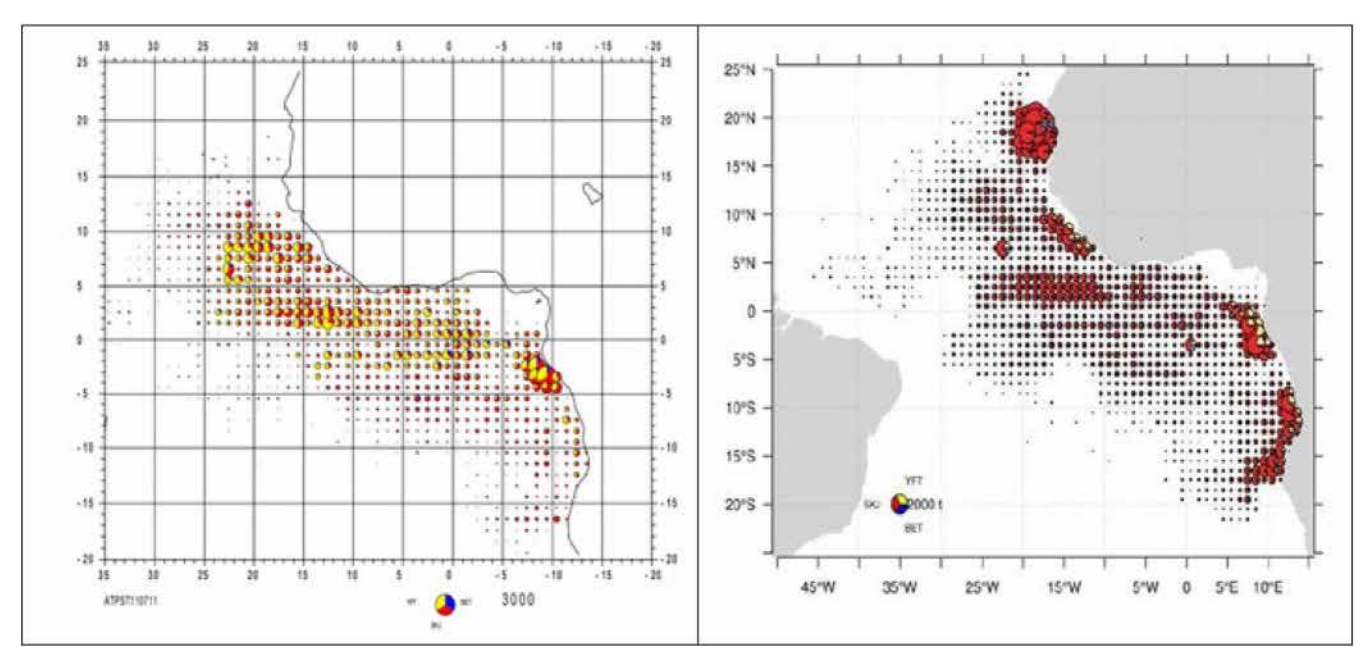


**FIGURE 1** | Distribution of average catches of Bigeye (BET), Skipjack (SKJ), and Yellowfin (YFT) tuna in the European purse-seine fleet in the eastern Atlantic Ocean during 2007–2011 (left panel; Delgado de Molina et al. 2014) and 2012–2016 (right panel; Pascual-Alayón et al. 2019).

subseries plots were developed as follows. First, for raw monthly catches, data were organized chronologically to ensure that monthly catches for each year from 1996 to 2019 were accurately compiled. For the percentage of monthly catch within a specific year, the cumulative annual catch was calculated first for every year in the dataset. Subsequently, the monthly catch was computed as a percentage of the yearly total for each month. Data from Task 2 of the ICCAT were used, excluding Belize and information on the composition (juveniles vs. others) of each species category for seasonal subseries plots. This approach allowed us to gather catch data for most flags and gears targeting tropical tuna associated with dFAD in the eastern Atlantic Ocean. In plots, the X-axis was months from January to December and the Y-axis was either raw monthly catches or the percentage of total annual catch. The plotting procedure vertically aligned data for each month over all 24 years (e.g., all January data points from 1996 to 2019 were stacked vertically, followed by February data, etc.). Raw monthly catches were disaggregated into four separate 6-year segments, and each segment was plotted using the same structure to detect seasonal variation over shorter periods. Consistency in peaks was used to identify months of consistently high catches across years. Temporal trends were scrutinized to detect increasing or declining temporal trends in catches and within 6-year subperiods. Short-term shifts in 6-year subperiods were examined to detect peak months or noticeable shifts in seasonality.

# 2.3 | Vector Autoregressive Spatiotemporal Model (VAST)

Fishery-dependent data provided non-random sampling of fish catches at specific locations that derived from a variety of unobserved spatial and temporal factors, including fish density and availability, management decisions such as time-area closures, and efficiency of fishing gear. Geostatistical modeling, particularly suitable for fishing data, incorporates spatial dependence through latent variables and spatially structured random effects to handle unbalanced designs (Monnahan et al. 2021). By sharing information across both space and time, models can address spatial cells missing data due to time-area closures like historic dFAD moratoria, as in the Eastern Atlantic Ocean (Thorson 2019; Xu et al. 2019).

To account for these spatiotemporal constraints, a vectorautoregressive spatiotemporal (VAST) delta-generalized linear mixed model was applied to catch and effort data using the VAST R package (Thorson 2019). VAST has superior performance over other standard methods, and maintains accuracy when data is incomplete for some areas within various combinations of years and seasons—a common problem with commercial catch data (Bryan and Thorson 2023; Grüss et al. 2019). Given these attributes, VAST is increasingly being used for CPUE standardization within tuna RFMOs (skipjack tuna in the Eastern Atlantic Ocean, Akia et al. 2022; yellowfin tuna in the Western Pacific Ocean, Vidal 2020; skipjack tuna in the Central Pacific Ocean, Vidal et al. 2020; yellowfin tuna in the Indian Ocean, Kitakado et al. 2021; and bigeye tuna caught by the longline fishery in the eastern Pacific Ocean, Satoh et al. 2021). VAST was initially developed by the Pacific Fisheries Management Council (PFMC) that manages fisheries in federal waters off the US West Coast (Thorson 2019), with early applications in the Pacific Ocean.

The VAST model used for our study was the "Poisson-link delta model", which employs a log-link function and a gamma distribution for its positive component (as indicated by ObsModel = c(2,1) in the R package VAST). The Poisson-link delta model used a probability distribution for catches B, with  $b_i$  the catch for purse-seine observation i (each purse seine observation corresponded to a set). The Poisson-link delta model included the probability  $p_i$  that observation i encountered a given

species [i.e., Pr(B > 0)], and the expected catch  $r_i$ , given that the species was encountered, Pr(B|B > 0):

$$\Pr(B = b_i) = \begin{cases} 1 - p_i & \text{if } B = 0\\ p_i G\{B | r_i, \sigma_m^2\} & \text{if } B > 0 \end{cases}$$
 (1)

where a gamma distribution G specified the distribution of positive catches (i.e., successful sets with a catch greater than 1 ton). This delta model predicted encounter probability  $p_i$  and positive catch rate  $r_i$  as a function of two linear predictors,  $\log(n_i)$  and  $\log(w_i)$ , for each observation i; and  $n_i$  and  $w_i$  were transformed to  $p_i$  and  $r_i$ :

$$p_i = 1 - \exp(-a_i n_i), \qquad r_i = \frac{a_i n_i}{p_i} w_i$$
 (2)

In the model,  $a_i$  was an offset variable that represented units of effort, expressed as the number of dFAD sets per observation. The expected density,  $d_i$  was the product of the encounter probability, the positive catch rate, and the transformed linear predictor,  $d_i = p_i \times r_i = n_i \times w_i$ . The model was defined as an expected density that was influenced additively by encounter probability and positive catch rate through a consistent log-link transformation:

mainly targeted dFAD, but both fleets expanded their use of dFAD more recently. In addition, the size category of vessels and a proxy for the modern technology introduced on board vessels (assuming old vessel were less equipped) likely played a role in choosing a fishing strategy. To account for this change, fleet country, vessel age, and vessel storage capacity (carrying capacity) were incorporated as catchability covariates (Table 1). Specifically, vessel age and vessel storage capacity were modeled as a three-degree polynomial spline using the bs function of the 'splines' R package (R Core Team 2021). Finally,  $\eta_{\rm n}(v_i)$  and  $\eta_{\rm w}(v_i)$  described random catchability variation between groups, as vessel identifiers, for each overdispersion factor. By combining Equations (3) and (4), densities for each extrapolation grid cell were determined by:

$$d(s,t) = n(s,t)w(s,t)$$
(5)

Overall abundance across the domain was then estimated as the area-weighted sum of density d(s, t) at a fine spatial resolution:

$$I(t) = \sum_{s=1}^{n_s} a(s)d(s, t)$$
 (6)

$$\log \operatorname{it}(n_i) = \underbrace{\begin{array}{c} \text{Temperal variation} \\ \beta_n(t_i) \end{array}}_{\beta_n(t_i)} + \underbrace{\begin{array}{c} \text{spatial variation} \\ \omega_n(s_i) \end{array}}_{} + \underbrace{\begin{array}{c} \text{spatiotemporal variation} \\ \varepsilon_n(s_i,t_i) \end{array}}_{} + \underbrace{\begin{array}{c} \text{catchability covariates} \\ \lambda_n(k)Q(i,k) \end{array}}_{} + \underbrace{\begin{array}{c} \text{vessel effects} \\ \eta_n(v_i) \end{array}}_{} (3)$$

The intercept parameters representing annual variation in the encounter rate  $(\beta_n)$  and positive catches  $(\beta_w)$  for the *i*th observation follow a first-order autoregressive (AR1) process. For the *i*th observation, spatial  $(\omega_n(s_i))$  and  $\omega_w(s_i)$  and spatiotemporal  $(\varepsilon_n(s_i,t_i))$  and  $\varepsilon_w(s_i,t_i)$  random effects accounted for residual variance not captured by fixed intercepts or covariates. Spatial and spatiotemporal effects were assumed to follow a multivariate normal distribution for encounter rate and positive catches. Covariance between locations was driven by a Matérn function, enhanced with geometric anisotropy, which allows decorrelation to vary between two directions. Spatiotemporal effects encompassed auto-correlation equations:  $\boldsymbol{\varepsilon}_{\mathrm{n}}(t) \sim \mathrm{MVN}(\rho_{\varepsilon_{\mathrm{n}}}\boldsymbol{\varepsilon}_{\mathrm{n}}(t-1), \mathbf{R}_{\mathrm{n}})$  $\boldsymbol{\epsilon}_{w}(t) \sim MVN(\rho_{\epsilon_{w}}\boldsymbol{\epsilon}_{w}(t-1), \boldsymbol{R}_{w})$ . Here,  $\boldsymbol{\epsilon}_{n}(t)$  and  $\boldsymbol{\epsilon}_{w}(t)$  denoted spatial variability vectors for encounter rate and positive catches in year t, with  $\mathbf{R}_n$  and  $\mathbf{R}_w$  being covariance matrices that incorporated a Matérn function for spatial decorrelation. Spatial variation described static, over-time variation in biomass density of tropical tuna, while spatiotemporal variation described yearly changes in biomass density for the Eastern Atlantic tropical tuna population. Temporal correlation of spatiotemporal components was described as an AR1 process to handle data from multiple sources (years with and without moratorium) and avoid unrealistic hot spots.

Parameters  $\lambda_n(k)$  and  $\lambda_w(k)$  represented catchability covariates to illuminate variables that affected the measurement process, but did not alter fish density. Historically, French purse seiners mainly targeted free schools, whereas Spanish purse seiners

where  $n_s$  was the number of extrapolation grid cell and  $a_s$  was the spatial area associated. The spatial area of each extrapolation grid was defined as 10,404 (102\*102) km² and 150 knots. Abundance indices were estimated as a spatial average of predicted density across the model extrapolation grid. Uncertainty of the index was estimated using a generalization of the delta method (Kass and Steffey 1989). In Equation (6),  $n_s$  was the total number of extrapolation grid cells and  $a_s$  was the associated spatial area. Model convergence was assumed when the gradient of the marginal log-likelihood declined below 0.0001 for all fixed effects and the Hessian matrix of second partial derivatives of the negative log-likelihood was positive definite

**TABLE 1** | Covariates in a model of tropical tuna catch-per-unit-of-effort for European purse-seiners (France and Spain) in the eastern Atlantic Ocean during 1996–2019.

Variable in the model	Description				
Fleet country	Fleet country: France and Spain				
Vessel age	The age of the vessel				
Numbat	Unique vessel identifier. Use as the random vessel effects variable				
Vessel storage capacity	Vessel storage capacity in m3				

(Grüss et al. 2020). Geostatistical analyses used R version 4.1.2 (R Core Team 2021). A model was fit for each of 12 months and 3 species during the 24-year period, for a total of 36 models. Data from European purse-seine fisheries operating in the Eastern Atlantic Ocean were used to standardize abundance indices and predict local catch density for each grid.

## 2.4 | Emerging Hotspot Analysis

Emerging hotspot analysis (EHSA) is a tool introduced by ArcGIS to detect spatiotemporal trends in data. By combining the Getis-Ord Gi\* statistic with the Mann-Kendall trend test, EHSA identifies trends in hot or cold spots over time (ESRI 2021). The goal of EHSA is to evaluate how hot and cold spots change over time to answer questions: are they becoming increasingly hotter, are they cooling down, or are they staying the same?

#### 2.4.1 | Gettis-Ord Gi\* Statistic

The Getis-Ord Gi\* is a prominent Local Indicator of Spatial Association (LISA) frequently employed in hotspot analysis such as crime mapping (Chainey and Ratcliffe 2013), epidemiology (Jimenez and Wongchanapai 2022; Rahman, Islam, and Islam 2021), environmental studies (Danek, Weglinska, and Zareba 2022; Ding et al. 2015), and real estate analysis (Downs 2004; Mondal 2020). Through computation of Gi\* statistics for spatial features (or spatial variable), the method discerns clustering intensity in regions with high values (hotspots) and low values (cold spots) in relation to a specific spatial variable (Chambers 2020; ESRI 2021) using the formula (Getis and Ord 1992; Ord and Getis 1995):

$$G_{i}^{*} = \frac{\sum_{j=1}^{n} \omega_{i,j} x_{j} - \overline{X} \sum_{j=1}^{n} \omega_{i,j}}{S \sqrt{\frac{\left[n \sum_{j=1}^{n} \omega_{i,j}^{2} - \left(\sum_{j=1}^{n} \omega_{i,j}\right)^{2}\right]}{n-1}}}$$
(7)

where  $x_j$  is the attribute for spatial feature j,  $\omega_{i,j}$  is the spatial weight between feature i and j, n is the total number of features, and

$$\overline{X} = \frac{\sum_{j=1}^{n} x_j}{n} \tag{8}$$

$$S = \sqrt{\frac{\sum_{j=1}^{n} x_{j}^{2}}{n} - (\overline{X})^{2}}$$
 (9)

## 2.4.2 | Mann-Kendall Trend Test

The Mann–Kendall trend test is widely used in various geoscience disciplines (Mann 1945). This non-parametric test evaluates the correlation between two variables based on the sequence order of the data, thereby discerning trends in long-term data series. The Mann–Kendall trend test statistic was calculated as follows:

$$S = \sum_{k=1}^{n-1} \sum_{j=k+1}^{n-1} sgn(x_j - x_k)$$
 (10)

where n is the length of the time series,  $x_j$  and  $x_k$  are values in the time series (j > k). "sgn" is a symbolic function, and

$$sgn(x_j - x_k) = \begin{cases} 1, & x_j - x_k > 0 \\ 0, & x_j - x_k = 0 \\ -1, & x_j - x_k < 0 \end{cases}$$
 (11)

The Mann-Kendall trend test uses a significance level of trend (Z) to test significance of the trend, and the slope of the trend (S) indicates degree and direction.

The statistic Z was calculated as follows:

$$Z = \begin{cases} \frac{S-1}{\sqrt{\text{VAR}(S)}} & S > 0\\ 0 & S = 0\\ \frac{S+1}{\sqrt{\text{VAR}(S)}} & S < 0 \end{cases}$$
 (12)

If Z > 0, the time series has a monodic upward trend, and if Z < 0, the time series has a monodic downward trend. Absolute critical values of Z are 2.576 for  $p \le 0.01$ , 1.06 for  $p \le 0.05$ , and 1.645 for  $p \le 0.1$ . Variance (S) was estimated as (Mann 1945):

VAR(S) = 
$$\frac{1}{18}[n(n-1)(2n+5)] - \sum_{p=1}^{q} t_p(t_p-1)(2t_p+5)(13)$$

where q is the number of sets with the same variable value, and  $t_p$  is the data number in the  $p_{th}$  set.

The EHSA tool requires a space–time NetCDF cube as input. For our analysis, we generated this by using the "Create Space–Time Cube by Aggregating Points" tool to build the required space–time NetCDF cube. EHSA uses Conceptualization of Spatial Relationships values to compute the Getis-Ord Gi\* statistic (Hot Spot Analysis) for each individual bin. Upon completion of the space–time hot-spot analysis, every bin in the input NetCDF cube was enriched with an associated z-score, *p*-value, and a classification of its hot-spot bin status. Following this, the Mann-Kendall trend test evaluated hot- and cold-spot trends. The outcome provided a trend z-score and *p*-value for each location with data, and the hot-spot z-score and *p*-value for every bin. The EHSA tool thereby categorized each location into hot- and cold-spot patterns (Appendix S1).

The Getis-Ord Gi\* statistic and hot-spot analysis were executed in Python and ArcGIS. Parameters for the analysis were as follows: a time step interval of 1 year, a space-time bin size of 102 km, and a neighborhood distance interval of 104 km. Primary data for creating the space-time NetCDF cube were spatiotemporal local biomass density, derived from standardization of catch per unit effort with VAST (Figure 2).

Before interpreting results from the EHSA, criteria for categorizing a region as a hotspot were defined. Regions characterized as Historical, Sporadic, Persistent, Intensifying, or Diminishing hotspots took precedence. These designations were pivotal because they highlighted areas that maintained a consistent hotspot presence of >90% throughout the study period. We focused

primarily on understanding clustering of tropical tunas, based on monthly local biomass density metrics from VAST for each tuna species. A specific region was pinpointed as an optimal moratorium zone if it persistently displayed hotspot patterns (historical, sporadic, persistent, intensifying, and diminishing) for either juvenile bigeye tuna or juvenile yellowfin tuna. This classification was especially pertinent during months when respective species demonstrated peak concentrations, as deduced from seasonal subseries plots.

## 2.5 | Moratorium Performance Metrics: Evaluating Actual ICCAT Strata Versus Suggested Optimum

To assist fishery managers and scientists in evaluating and comparing effectiveness of ICCAT and proposed new moratorium strata, two objective metrics based on monthly biomass density data were developed to determine the most effective moratorium strata for protecting juvenile bigeye and yellowfin tuna. First, a standardized efficiency index was computed for each moratorium area by dividing the total monthly catch in the area by the number of squares within that area and for the entire fishing region:

$$\text{ME}_{\text{New\_area}} = \frac{\sum_{k=1}^{\text{number of grids}} \text{local biomass density in the new moratorium area}}{\sum \text{number of grids cover by the new moratorium area}}$$

$$\mathrm{ME}_{\mathrm{Actual\_area}} = \frac{\sum_{k=1}^{\mathrm{number\ of\ grids}} \mathrm{local\ biomass\ density\ in\ the\ actual\ moratorium\ area}}{\sum \mathrm{number\ of\ grids\ cover\ by\ the\ actual\ moratorium\ area}}$$

$$\text{ME}_{\text{Fishing\_area}} = \frac{\sum_{k=1}^{\text{number of grids}} \text{local biomass density in the entire fishing area}}{\sum \text{number of grids cover by the entire fishing area}}$$

#### 2.5.1 | Moratorium Efficiency Ratio (MER)

A Moratorium Efficiency Ratio metric was designed to identify the most effective moratorium area for protecting juvenile bigeye or yellowfin tuna. The metric involves a comparative analysis of monthly mean biomass density of these species within two distinct moratorium areas. The local biomass density, assessed per local square grid using the VAST method, was summed and divided by the total number of grids in both moratorium areas:

$$MER = \frac{ME_{New\_area}}{ME_{Actual\_area}}$$

The resulting ratio of these indices was then compared to a benchmark value of 1. If MER > 1, the moratorium was more efficient than the ICCAT moratorium.

## 2.5.2 | Moratorium Performance Index (MPI)

A Moratorium Performance Index was used to compare average biomass density within the moratorium zone to the entire fishing area. The MPI contrasted monthly mean biomass density within the moratorium area to that of the larger fishing region. This comparison generated two indices to enable evaluation of the effectiveness of either the current or proposed moratorium stratum in terms of biomass density:

$$MPI_{Optimum} = \frac{ME_{New\_area}}{ME_{Fishing\_area}}$$

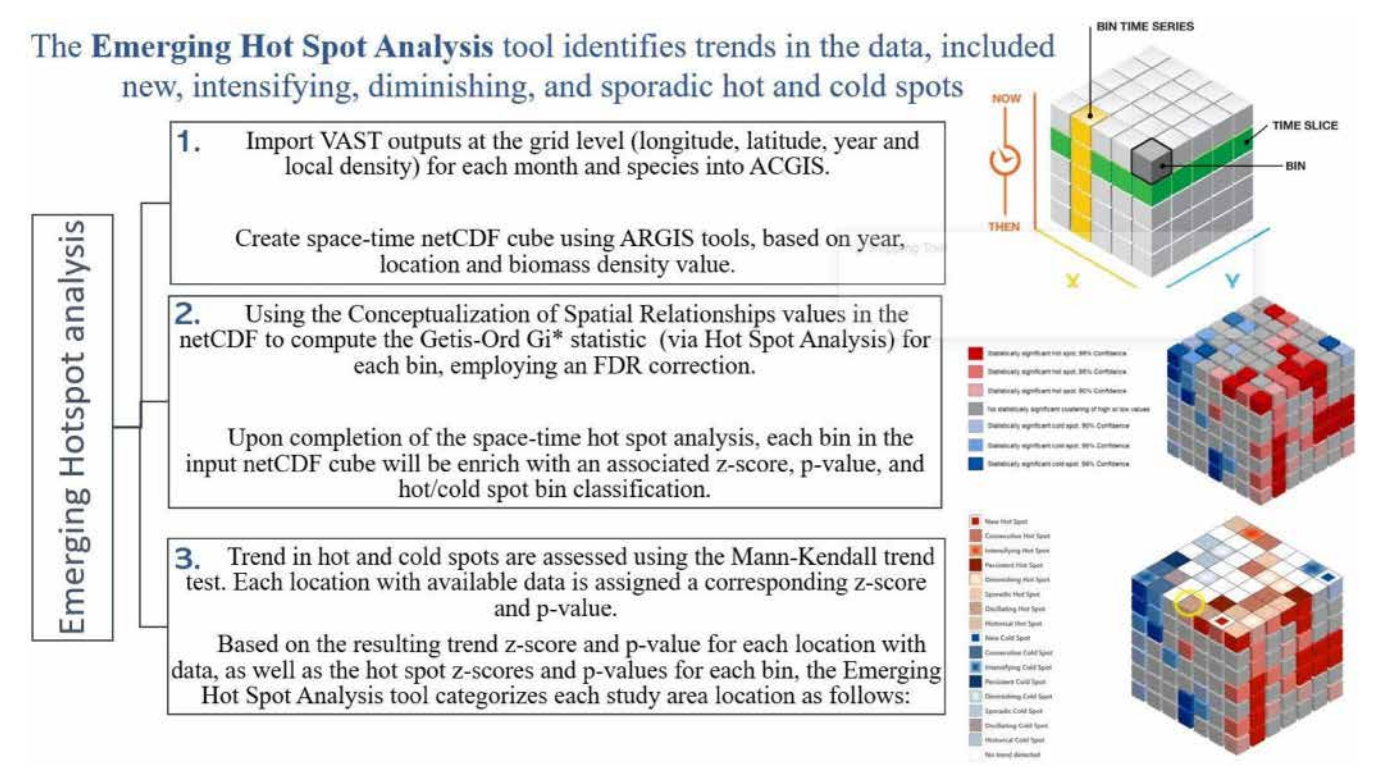


FIGURE 2 | Flowchart detailing the step-by-step procedure for emerging hotspot analysis, illustrating sequential methodologies and decision points essential for accurate spatial trend identification.

$$MPI_{Actual} = \frac{ME_{Actual\_area}}{ME_{Fishing\_area}}$$

If  $MPI_{Optimum} > MPI_{Actual}$ , the moratorium was more efficient than the actual moratorium.

The analysis contrasted actual ICCAT moratorium areas with suggested moratorium areas, based on relevant months. These metrics collectively provided a systematic approach to identify the most appropriate moratorium strata.

#### 3 | Results

#### 3.1 | Seasonal Subseries Plots

Seasonal subseries plots demonstrated pronounced seasonality in monthly catches of all three tuna species. Juvenile bigeye tuna mainly exhibited peaks in the first and last quarters, with a discernible surge beginning in September for the final quarter (Figure 3). Although the 5-year data showcased some variability in monthly patterns across most years, monthly catches clearly ebbed and flowed in percentages. This fluctuation suggested an underlying trend in the data that transcended obvious seasonality. This trend was also apparent for the other two tuna species, with juvenile yellowfin tuna peaking from August to December and skipjack tuna peaking from July to December (Figures 4 and 5).

## 3.2 | VAST Results

The spatiotemporal models for both BET and YFT successfully converged, as confirmed by maximum gradient component values smaller than 0.0001 (Appendix S2, Table S1) and a positive definite Hessian matrix, ensuring the accurate estimation of key model parameters. The VAST model outputs provide log-predicted density estimates for each species across the study period and for each extrapolation grid (102 km × 102 km), representing the spatiotemporal local biomass density. These spatiotemporal local biomass densities, as shown for some species-month combinations in Appendix S2 (Figures S1-S4), were subsequently used to create the space-time NetCDF cube in the Emerging Hotspot Analysis. Furthermore, the residual diagnostics suggest a good fit to the catch and effort data. The QQ plots, which assess deviations between observed and theoretical distributions, show points mostly falling close to the diagonal, indicating that the model residuals follow a normal distribution, with minor deviations in the tail data (Appendix S2, Figures S5-S10). Residual plots against covariates, including age, storage capacity, year, and knot\_ID, reveal no significant patterns, further supporting the robustness of the models (Appendix S2, Figures S5-S10).

## 3.3 | Emerging Hotspot Analysis

From January to March, juvenile bigeye tuna were distinctly concentrated, with a peak in February (Figure 6). The February peak was encompassed by diminished hotspot areas

in January and March. The first quarter was a prime moratorium period for juvenile bigeye tuna, as indicated by the hotspot distribution in February. The critical area of interest during this period extended from 6°W to 6°E longitude and from 9°S to 1°N latitude, a region that corresponded closely with prominent hotspots for skipjack tuna and juvenile yellowfin tuna. Notably, yellowfin tuna did not peak during this period. Establishment of a moratorium in this zone during the first quarter could substantially reduce bigeye catches, particularly those associated with skipjack tuna under dFAD. Furthermore, a moratorium in the area would reduce juvenile yellowfin captures, while also reducing skipjack catches. To enhance effectiveness of the moratorium, another area of overlapping hotspots of the three tuna species could be integrated into the primary zone from 27°W to 15°W longitude and 1°N to 7°S latitude from April to August (Appendix S3, Figures S2, S3). However, because catches of juvenile bigeye and yellowfin tuna were lower in these months, these spots were not prioritized for protection of these young fish. Juvenile bigeye tuna were concentrated from September to November, when they overlapped with concentrations of juvenile yellowfin and skipjack tuna (Figures 7 and 8). Juvenile yellowfin tuna were concentrated in area from 25°W to 5°E longitude and 8°S to 2° N latitude (Figure 8). The Gabonese coast was a hotspot for yellowfin tuna, although more localized than for the other two species. The Gabonese coast was particularly significant as a viable moratorium target area for juvenile yellowfin, although yellowfin were associated with skipjack under dFAD.

## 3.4 | Moratorium Performance Metrics

The Moratorium Efficiency Ratio (MER) and Moratorium Performance Index (MPI) suggested that the newly developed moratorium would reduce catches of BET and YFT and outperform ICCAT recommendations during 1999–2019 (Figures 9, 10, Tables 2 and 3). The reduction in BET catches was generally more significant than YFT, except for Rec11, where the difference in reduction was smaller. Proposed moratorium zones could be unsuccessful for protecting juvenile BET and YFT, but still permit fishing of SKJ during moratorium periods.

#### 4 | Discussion

We identified two key zones, each optimal during distinct months, as the most suitable for moratorium implementation, which relatively closely aligned with existing ICCAT large spatial closures to surface gear fishing on FADs in the Gulf of Guinea (ICCAT Recommendations 04–01, 08–01, 11–01, 14–01, 15–01 for the first 2 and the last 2 months of the year, and the entire Atlantic 19–01, 22–01 from January 1 to March 13). However, our suggested zones were more concentrated in the Guinean Gulf, in contrast with the existing moratorium that covers a vast stretch of the African coast or all of the Atlantic Ocean. Another distinction was related to the recommended duration of the moratorium of 3–4 months, rather than 2–3 months.

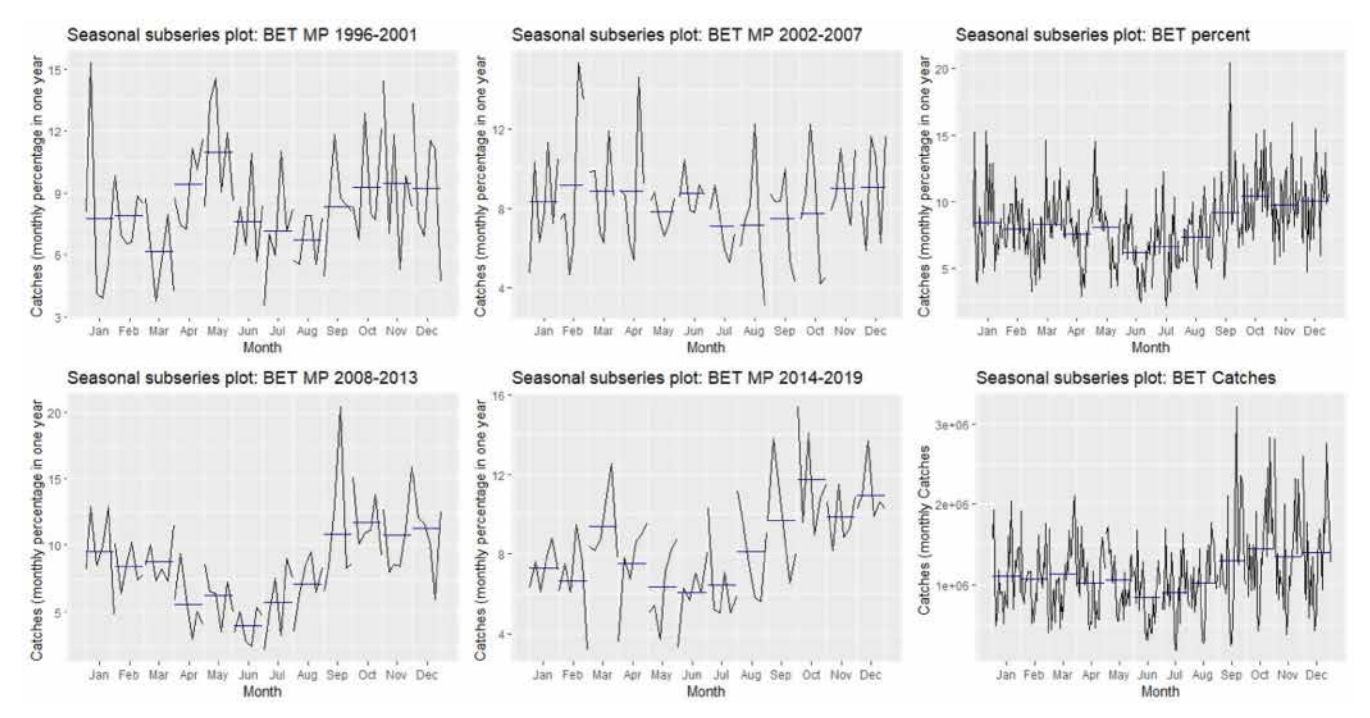


**FIGURE 3** | Seasonal catches of bigeye tuna (BET) in European Eastern Atlantic purse seine fisheries during 1996–2019. The left and central panels display monthly percentages of yearly catches (MP) in four 5-year intervals. The right panel aggregates the entire period, with the top plot showing the MP and the bottom detailing monthly catches. Horizontal lines represent the monthly averages, and vertical lines highlight deviations from these averages for each year.

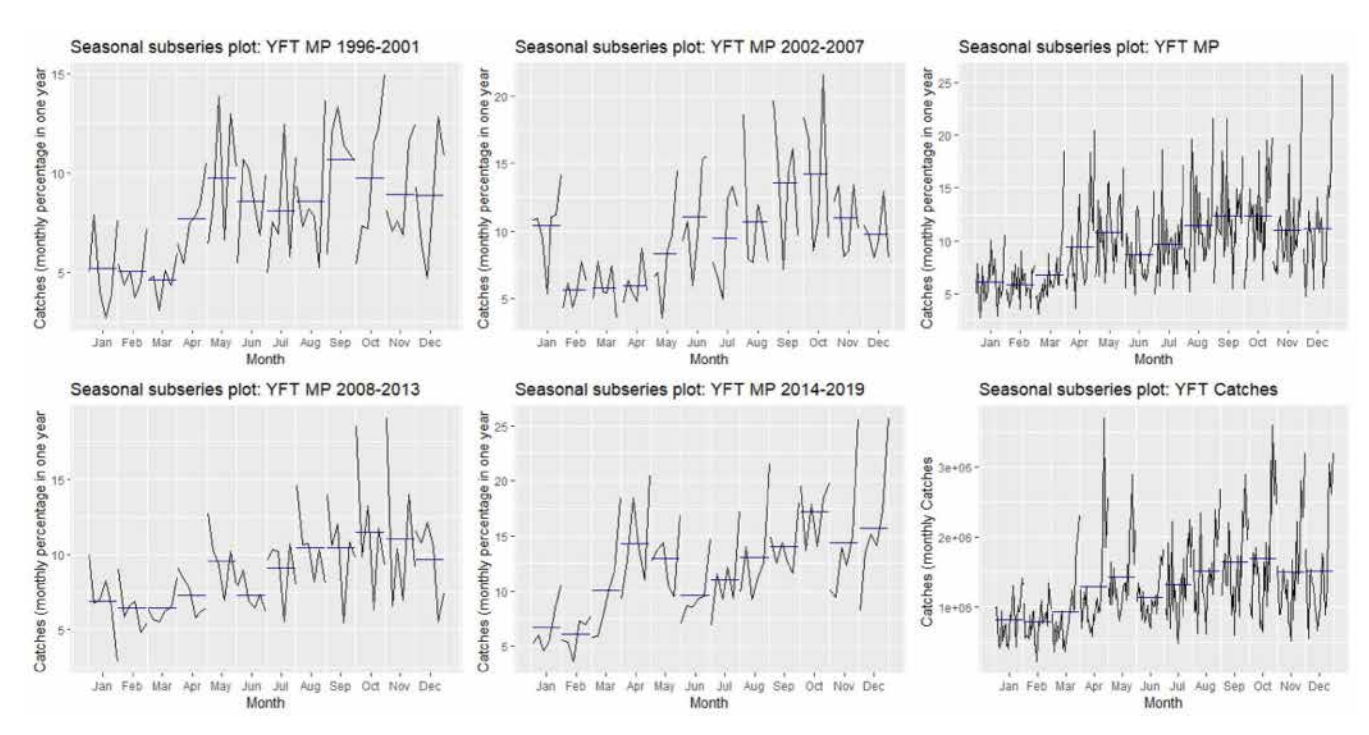


**FIGURE 4** | Seasonal catches of yellowfin tuna (YFT) in European Eastern Atlantic purse-seine fisheries during 1996–2019. Left and central panels display monthly percentages of yearly catches (MP) in four 5-year intervals. The right panel aggregates the entire period, with the top plot showing the MP and the bottom detailing monthly catches. Horizontal lines represent the monthly averages, and vertical lines highlight deviations from these averages for each year.

We introduced a dynamic method for identifying hotspot areas that was crucial for protecting juvenile tuna, which is essential for sustaining fish populations by ensuring ecological balance and maximizing economic returns (Vasilakopoulos, Oneill, and Marshall 2011). High fishing mortality of immature fish significantly harms stock status (Vasilakopoulos, Oneill, and

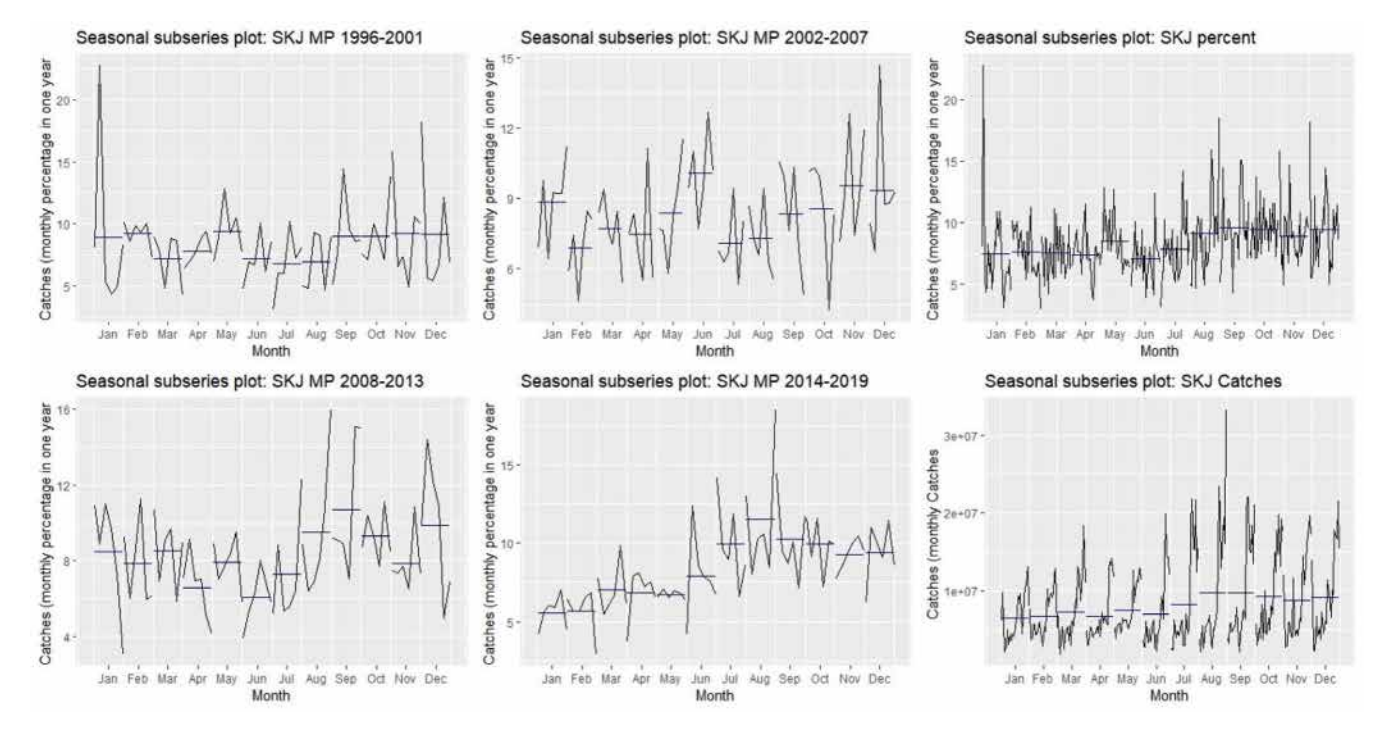


**FIGURE 5** | Seasonal catches of skipjack tuna (SKJ) in the European Eastern Atlantic purse seine fisheries from 1996 to 2019. Left and central panels display monthly percentages of yearly catches (MP) in four 5-year intervals. The right panel aggregates the entire period, with the top plot showing the MP and the bottom detailing monthly catches. Horizontal lines represent the monthly averages, and vertical lines highlight deviations from these averages for each year.

Marshall 2011). A meta-analysis of 38 fish stocks across 13 species in the Northeast Atlantic revealed that a mortality rate on immature fish exceeding half of mature fish caused stock status to fall below precautionary limits (Vasilakopoulos, O'Neill, and Marshall 2012). This finding highlights the importance of allowing fish to spawn at least once before they are subjected to fishing, to prevent recruitment overfishing and support stock recovery. Real-world examples reinforce the importance of juvenile protection, such as the collapse of the Northern cod (Gadus morhua) stock in the Northwest Atlantic (Bundy 2001; Rose and O'Driscoll 2002). Conversely, recovery of Atlantic Bluefin Tuna in the Atlantic Ocean was facilitated by a ban on fishing bluefin tuna below spawning age and increasing the minimum size to 30kg (Bjørndal 2023). This measure allowed many tunas born in the Mediterranean, which migrate to feed in areas like the Bay of Biscay, to survive and return to spawn, saving over a million fish annually (Planet Tuna 2020).

While developing the methodology for this study, we faced a crucial decision between two modeling approaches for estimating local fish density, each of which significantly affected the effectiveness of our hotspot analysis. A seasonal VAST model aggregated data into seasonal (monthly) factors to account for variability within and across years (Thorson et al. 2020), thereby resulting in fewer models (one per species). In contrast, a month-by-month approach, with 12 models per species, offered finer temporal resolution, by isolating each month, to capture subtle, long-term changes in spatial distribution (Alglave et al. 2023, 2024; Pinto et al. 2019) crucial for identifying emerging hotspots at a monthly scale.

This latter approach assumed that temporal correlation between the same month in different years was stronger and more meaningful than between consecutive months within the same year, by isolating each month and focusing solely on yearly dynamics, due to recurring seasonal processes. In spatiotemporal models, using the AR1 process for annual intercepts and spatiotemporal component allowed us to better capture recurring dynamics by modeling temporal correlations (Thorson 2019). We hypothesize that consistent ecological conditions in the same month across different years provided a more accurate explanation of fish density than month-to-month comparisons within the same year. This is particularly relevant for tropical tunas, where the identification of monthly or seasonal moratorium periods is crucial. Therefore, we opted for a 12-model per species approach to align with our hypothesis, by focusing exclusively on intraannual monthly series rather than combining both intra- and inter-annual correlations. While our modeling choice can be debated, our results support a month-by-month approach with AR1 process that has produced more reliable and nuanced fish density estimates, particularly in areas with irregular sampling due to moratoriums. Spatial distributions of significant emerging hotspots, especially in February and January for BET, indicated patterns driven by consistent seasonal processes. The strong relationship we found between January and February distributions shifted in March. Additionally, the observed seasonality in significant hotspots may be influenced by factors such as seasonal recruitment, presence of specific juvenile habitats, or fleet behavior, including deployment of dFADs in the fishing area.

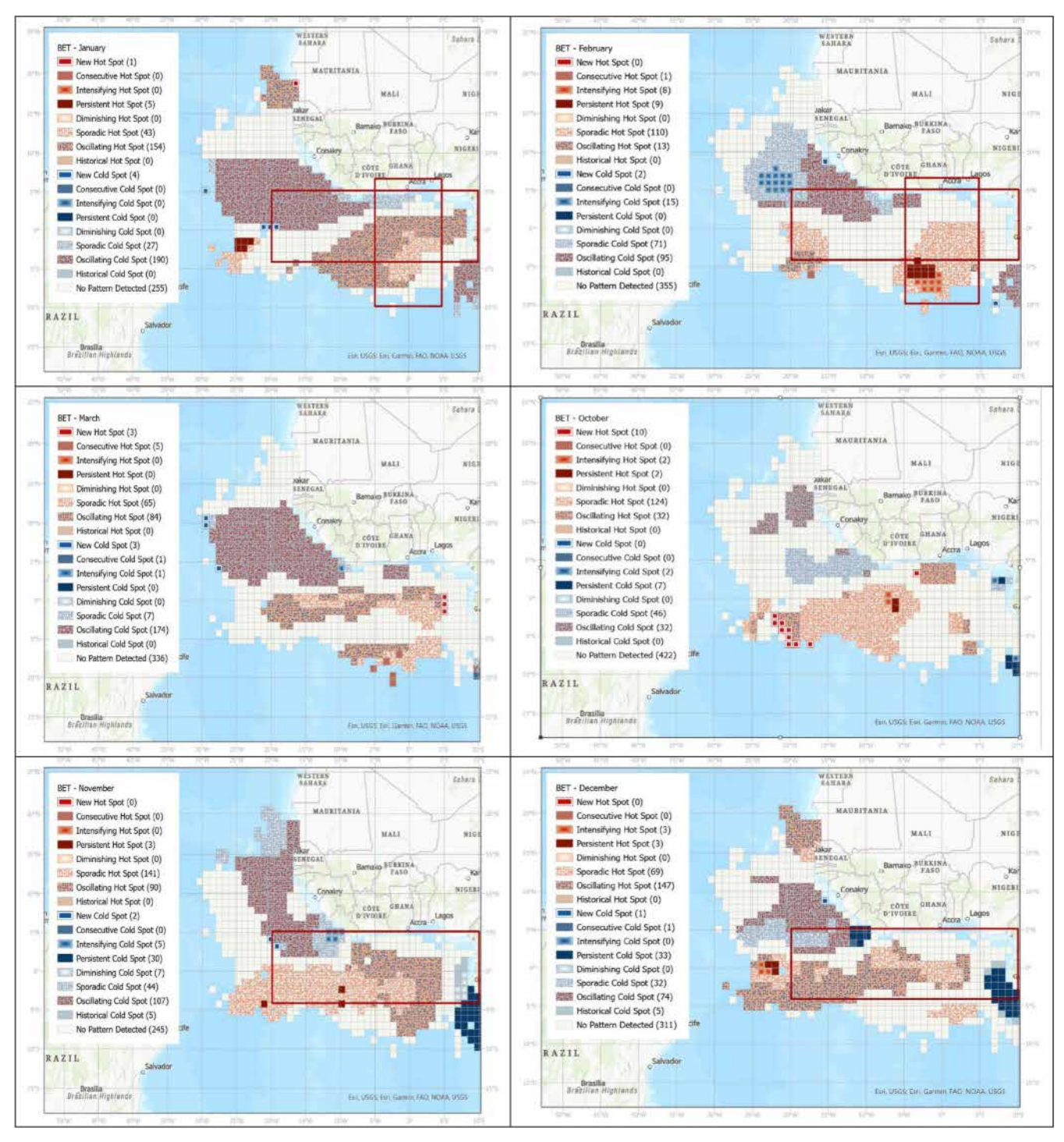


FIGURE 6 | Monthly hotspots of bigeye tuna catches, highlighting areas with significant spatial trends, in European purse-seine (France and Spain) fisheries in the eastern Atlantic Ocean in January, February, March–October, and November–December, during 1996–2019. The included legend details the main categories and patterns observed in the analysis, with accompanying numbers indicating the frequency of each pattern in the displayed results. Regions characterized as Historical, Sporadic, Persistent, Intensifying, or Diminishing hotspots (all categories in shades of red) are considered significant hotspots to be considered within this figure. Red boxes highlight the current ICCAT moratorium zone for the respective month.

Biological cycles, environmental conditions, and fishing practices, particularly use of FADs, all play critical roles in defining seasonal patterns we identified for catches of tuna species were corroborated by earlier studies. For example, bycatch of skipjack tuna was highest in the third and fourth quarters due to intensive FAD use, with a peak in the third and fourth quarters (Amandè et al. 2010). Similarly, catches of juvenile yellowfin tuna were highest from August to November

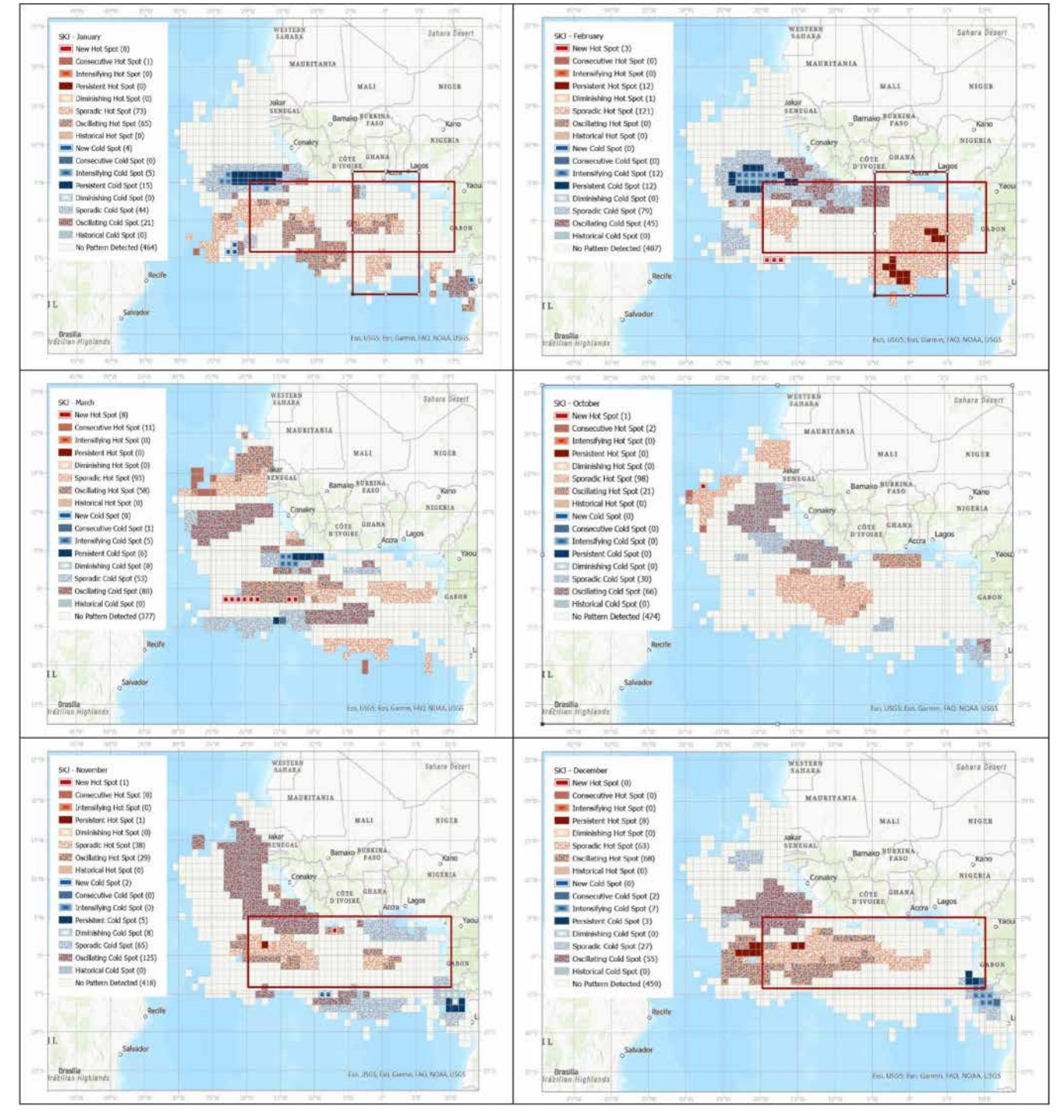


FIGURE 7 | Monthly hotspots of skipjack tuna catches, highlighting areas with significant spatial trends, in European purse-seine (France and Spain) fisheries in the eastern Atlantic Ocean in January, February, March October, November and December during 1996–2019. The included legend details the main categories and patterns observed in the analysis, with accompanying numbers indicating the frequency of each pattern in the displayed results. Regions characterized as Historical, Sporadic, Persistent, Intensifying, or Diminishing hotspots (all categories in shades of red) are considered significant hotspots to be considered within this figure. The red boxes highlight the current ICCAT moratorium zone for the respective month.

(Druon et al. 2015). Seasonality in bigeye tuna catches we found during the first and fourth quarters aligns with spawning cycles and juvenile availability in the region (Schirripa 2016). Seasonal patterns identified in our study are supported by biological

and environmental factors affecting tropical tuna in this area (Fonteneau and Marcille 1993). Increased deployment of FADs during specific periods significantly impacts the distribution and catch rates of juvenile tuna species, particularly skipjack and

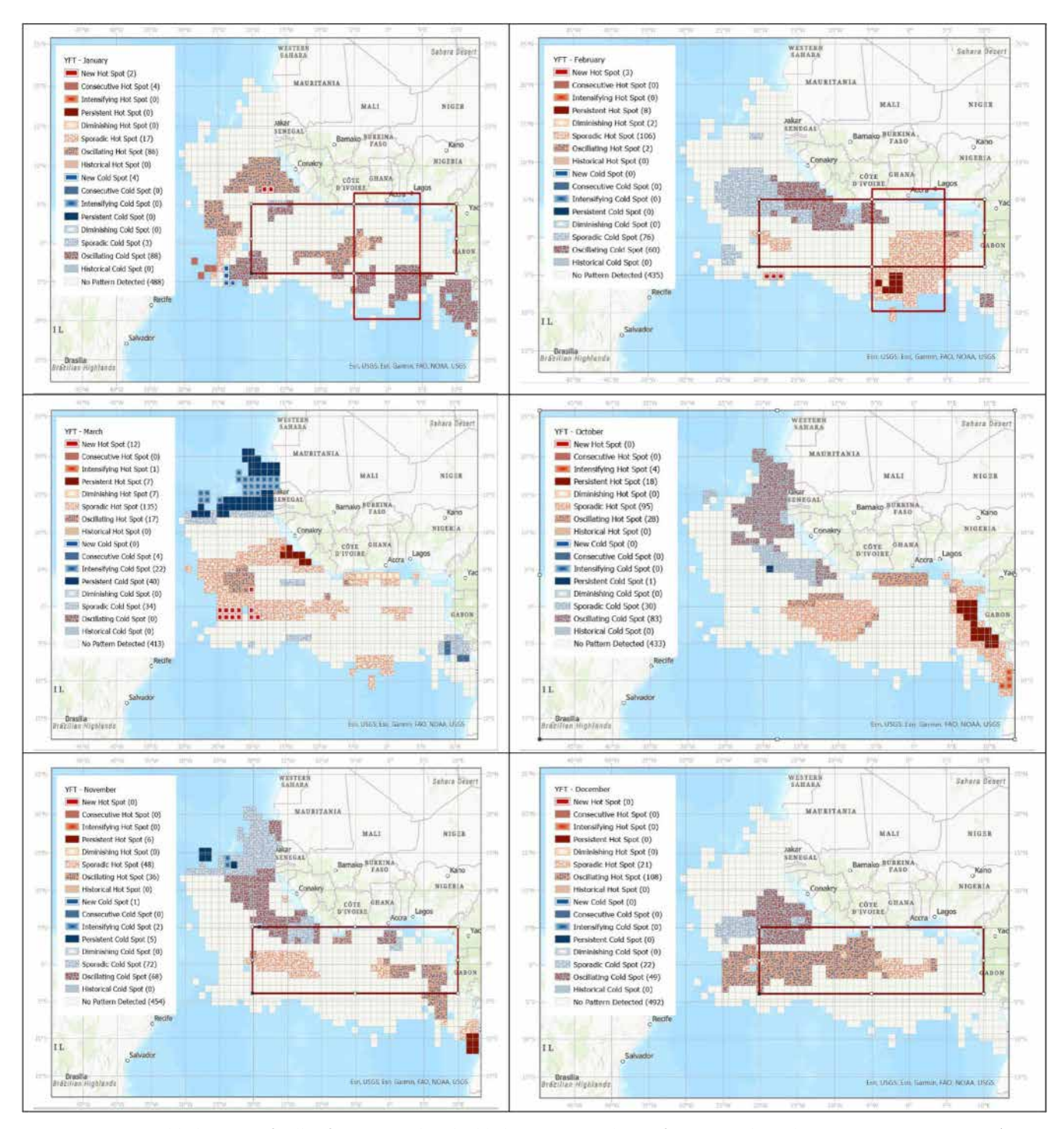


FIGURE 8 | Monthly hotspots of yellowfin tuna catches, highlighting areas with significant spatial trends, in European purse-seine (France and Spain) fisheries in the eastern Atlantic Ocean for January, February, March October, November and December during 1996–2019. The included legend details the main categories and patterns observed in the analysis, with accompanying numbers indicating the frequency of each pattern in the displayed results. Regions characterized as Historical, Sporadic, Persistent, Intensifying, or Diminishing hotspots (all categories in shades of red) are considered significant hotspots to be considered within this figure. The red boxes highlight the current ICCAT moratorium zone for the respective month.

yellowfin tuna (Hallier and Gaertner 2008; Pérez et al. 2020). Biological factors such as spawning periods and subsequent juvenile migration patterns are key drivers of the observed seasonality in juvenile yellowfin and bigeye tuna catches (Fonteneau

and Marcille 1993). Seasonal changes in oceanographic conditions are crucial in defining the habitats and migration routes of these species (Druon et al. 2017; Fonteneau and Marcille 1993; Lopez et al. 2017).

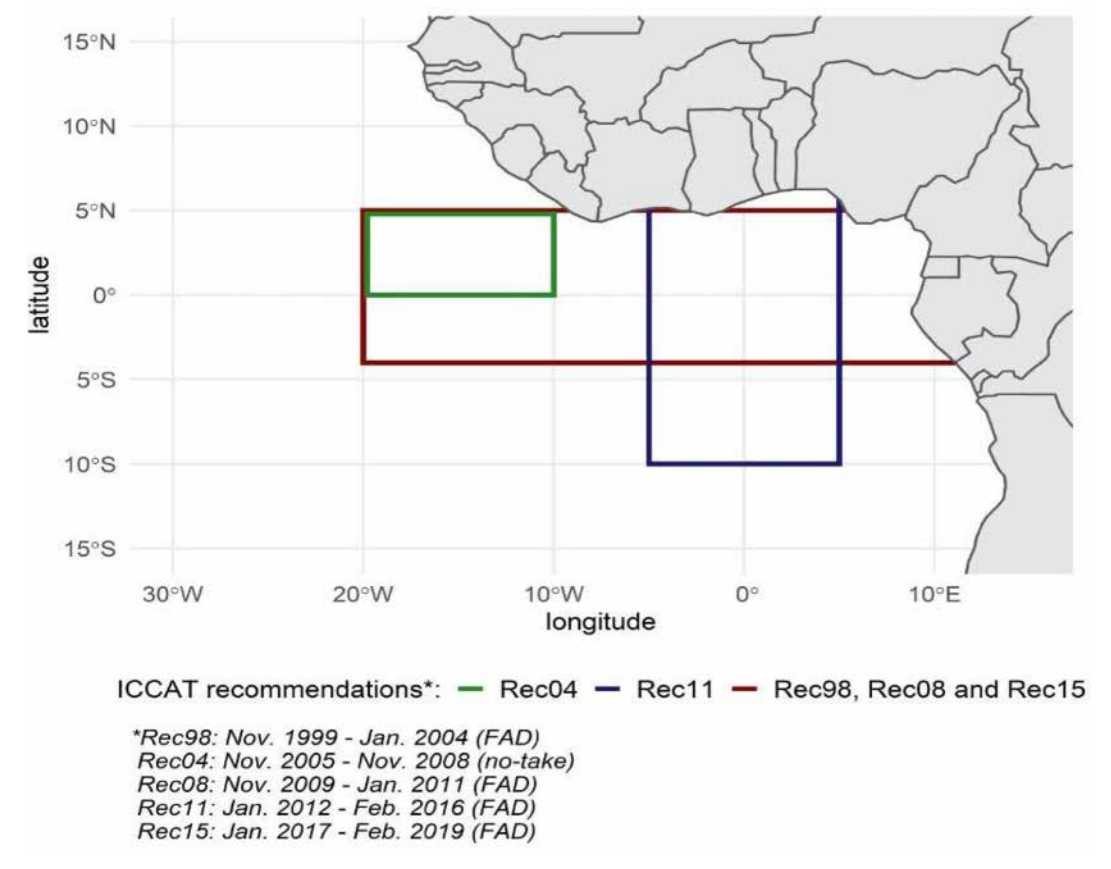


FIGURE 9 | ICCAT recommended closed areas for European tropical tuna purse-seine (France and Spain) fisheries in the eastern Atlantic Ocean since their introduction in 1999 to 2019 (from Stephan et al. (2022)). The figure illustrates the geographical areas in the eastern Atlantic Ocean where ICCAT implemented management recommendations during this period, focusing on the regulation of Fish Aggregating Devices (FADs) through time-area closure measures aimed at conserving juvenile of BET and YFT along with other species impacted by FAD fishing. Colored boxes represent specific management areas, and "Rec" numbers correspond to the relevant recommendation periods. The Blue Box (Rec11) for example highlights the regulation of FADs between January 2012 and February 2016.

Despite different spatial structuring of habitat and temporal structuring of food chains, marine resource management has tended to rely on concepts inherited from terrestrial resource management, such as use of static marine protected areas (Maxwell et al. 2015). While static approaches can work for relatively stationary marine resources, highly migratory tunas and great mobility of industrial fleets would seem to support greater flexibility in the definition of spatiotemporal strata used by managers to regulate fisher access or practice (e.g., ban of dFAD-fishing). For example, simulated closures across a range of spatiotemporal scales showed that coarse-scale management measures (i.e., annual time area closures and monthly full-fishery closures) required 100-200 times more km<sup>2</sup>-days of closure than dynamic measures, such as grid-based closures and move-on rules, to achieve similar reduction in juvenile bycatch (Dunn et al. 2016). Similarly, a multispecies predictive habitat modeling framework, combined with satellite telemetry and fisheries observer data, to estimate species-specific probabilities of occurrence, suggested that dynamic closures could be 2-10 times smaller than existing static closures to still adequately protect endangered non-target species (Hazen et al. 2018).

Predictions from an SDM based on probability of Southern Bluefin Tuna (Thunnus maccoyii) occurrence were used by managers to regulate fisher access to the areas where this species is abundant (Hobday et al. 2010). A similar approach based on species distribution and habitat modeling was used to evaluate whether an existing closed areas on U.S. Atlantic coasts was appropriately placed to achieve ongoing conservation and management objectives and did not unnecessarily prevent fisheries from attaining optimum yield from healthy fish stocks (Crear et al. 2021). However, although identification of habitat preferences for protecting a species or age-class is valuable, use of SDM may be limited by climate change, as when an explanatory variable changes beyond the range used in the model (Porfirio and Harris, 2014), by lack of model validation in no-take zones, as when other candidate explanatory variables not used in the model may have a local impact (Yates et al., 2018), or by the fact that co-occurrence between species may not be extrapolable (Dormann et al. 2018). Because optimal habitats for mobile species can change within and between years, use of SDM in dynamic ocean management (DOM) is a logical next step, in which real-time data are used to generate spatial management measures that can change across space and time in response to



**FIGURE 10** | Recommended Moratorium Areas for European tropical tuna purse-seine (France and Spain) fisheries in the eastern Atlantic Ocean. The blue zone indicates a proposed moratorium period from September to November, while the green zones represent proposed moratorium periods from January to March.

environmental variability (Hobday et al. 2014). However, a gap between choice of the optimal scientific method and feasibility of its application may hinder the decision-making process. The best option of DOM would be to account for environmental variability at the time of implementation of a moratorium (i.e., real-time management), but is difficult to set within the framework of tuna RFMOs. For management recommendations to be applicable by all CPCs, the space–time closure stratum should

TABLE 2 | Moratorium Efficiency Ratio (MER) for Bigeye (BET), Skipjack (SKJ), and Yellowfin (YFT) tuna for European purse-seine (France and Spain) fisheries in the eastern Atlantic Ocean during 1996–2019. An ICCAT Recommendation (Rec) is a binding decision on conservation and management measures for tuna species, adopted by the ICCAT Commission. Rec 98 for BET refers to specific recommendations issued in 1998 for a BET.

	BET	SKJ	YFT
Rec 98	1.333	1.049	1.125
Rec 08	1.220	1.030	1.038
Rec 11	1.076	1.040	1.076
Rec 15	1.295	1.098	1.058

be set in advance, at the time of the Annual Commission (i.e., at year n), on a "stable" basis that cannot be modified during the year when the measure is implemented (year n+1). This limits implementation of a DOM approach in tuna RFMOs, but does not preclude establishment of smaller seasonal strata that are mobile from one season to the next. One challenge policymakers face is comparing effectiveness of a large static area regulated for a short period of time with several mobile smaller areas regulated for a longer time.

One criticism of the effectiveness of time and area closures is that tuna fleets can simply redistribute effort outside a moratorium area, without significantly reducing total fishing effort (Fonteneau et al. 2016). For example, higher dFAD catches during the first ICCAT moratorium close to boundaries of the restricted area suggested a potential "fishing the line effect" (Torres-Irineo et al. 2011), but a similar phenomenon was not evident in waters adjacent to the following moratoria (Perez et al. 2022). Obviously, the impact of effort re-allocation must always be considered when planning deployment of time-area closures (Hilborn et al. 2004). In addition, effective implementation of dynamic closures must account for other aspects linked with characteristics of the tuna resource, such as migratory patterns of each tuna species and home range size of individual fish relative to size of the closed area (Kaplan et al. 2014).

TABLE 3 | Moratorium Performance Index (MPI) for Bigeye (BET), Skipjack (SKJ), and Yellowfin (YFT) tuna for European purse-seine (France and Spain) fisheries in the eastern Atlantic Ocean during 1996–2019. A comparative analysis of the moratoriums defined in various ICCAT recommendations (1999–2019) (ICCAT Rec) versus the new proposition using spatiotemporal methods from this study (New). An ICCAT Recommendation (Rec) is a binding decision on conservation and management measures for tuna species, adopted by the ICCAT Commission. Rec 98 for BET refers to specific recommendations issued in 1998 for a BET.

	ВЕТ		SKJ		YFT	
	ICCAT Rec	New	ICCAT Rec	New	ICCAT Rec	New
Rec 98	1.097	1.463	0.665	0.697	1.196	1.346
Rec 08	0.752	0.918	0.604	0.622	0.852	0.885
Rec 11	1.202	1.294	1.078	1.122	1.032	1.111
Rec 15	1.059	1.371	1.024	1.125	1.035	1.097

## 5 | Conclusions

We found that dFAD moratorium stratum should be divided into several smaller mobile areas spread over the last 3-4 months of the year, unlike the current ban on dFAD fishing in a very large area for only a couple of months, which does not seem to be effective and may not be accepted as necessary by CPCs in the development of management measures. This could even be used to reject any area-based management regulation, although spatial and temporal locations of the current moratoria have never been scientifically studied. Implementation of moratoria on dFAD is not a panacea and should be combined with other fisheries management measures, as in the tropical Atlantic, where the fishery is regulated by catch limits, limits on the number of buoys monitored by a purse seiner at any time, and limits on the number of support vessel per purse seiner. Despite the multispecies nature of the tropical tuna fishery, implicitly recognized in the title of the ICCAT recommendations (i.e., "On a multi-annual conservation and management program for tropical tunas"), the bigeye tuna is the species with the worst stock health status, and therefore the main species targeted by protection measures. Consequently, the most efficient management measures should control mortality on both juveniles and adults, through prohibition of fish aggregation devices in the purse-seine fishery and restrictions on longline fishing in spawning areas (Sibert et al. 2012). Instead of restricting use of a specific gear (longlines) or a specific fishing method (dFAD) over a large area for a short part of the year, fragmenting the regulation area into several smaller mobile zones over a longer part of the year would be an interesting alternative to protect juveniles or spawners.

## Acknowledgements

We sincerely thank the contribution of the staff of the Ob7-IRD for providing data on the French fleet and the staff of the Instituto Español de Oceanografía for providing data on the Spanish fleet.

#### **Conflicts of Interest**

The authors declare no conflicts of interest.

#### **Data Availability Statement**

The data used for the spatiotemporal model and Emerging Hotspot analysis were provided by Ob7-IRD staff for the French fleet and IEO (Instituto Español de Oceanografía) staff for the Spanish fleet, and can be earned by requesting these two institutes. The data used for the seasonal subseries plots included ICCAT Task 2, which can be accessed at https://www.iccat.int/en/accesingdb.html.

#### References

Akia, S., L. Guery, M. Grande, et al. 2022. "European Purse Seiners CPUE Standardization of Eastern Atlantic Skipjack Caught Under Non-OWNED DFADS Using the Vast Methodology." *Collective Volume of Scientific Papers ICCAT* 79, no. 1: 210–221.

Alglave, B., M. Olmos, J. Casemajor, et al. 2024. "Investigating Fish Reproduction Phenology and Essential Habitats by Identifying the Main Spatio-Temporal Patterns of Fish Distribution." *ICES Journal of Marine Science* 81: 1563–1574. https://doi.org/10.1093/icesjms/fsae099.

Alglave, B., Y. Vermard, E. Rivot, M.-P. Etienne, and M. Woillez. 2023. "Identifying Mature Fish Aggregation Areas During Spawning Season by Combining Catch Declarations and Scientific Survey Data." *Canadian Journal of Fisheries and Aquatic Sciences* 80, no. 5: 808–824. https://doi.org/10.1139/cjfas-2022-0110.

Amandè, M. J., J. Ariz, E. Chassot, et al. 2010. "Bycatch of the European Purse Seine Tuna Fishery in the Atlantic Ocean for the 2003-2007 Period." *Aquatic Living Resources* 23, no. 4: 353–362. https://doi.org/10.1051/alr/2011003.

Ariz, J., A. Delgado, A. Fonteneau, F. Gonzales Costas, and P. Pallarés. 1999. "Logs and Tunas in the Eastern Tropical Atlantic: A Review of Present Knowledge and Uncertainties." In *Proceedings of the International Workshop on the Ecology and Fisheries for Tunas Associated with Floating Objects. Presented at the Inter-American Tropical Tuna Commission Special Report 11, La Jolla, CA (1999)*. edited by M.D. Scott, W.H. Bayliff, C.E. Lennert-Cody, and K.M. Schaefer, 21–65.

Bjørndal, T. 2023. "The Northeast Atlantic and Mediterranean Bluefin Tuna Fishery: Back From the Brink." *Marine Policy* 157: 105848. https://doi.org/10.1016/j.marpol.2023.105848.

Bryan, M. D., and J. T. Thorson. 2023. "The Performance of Model-Based Indices Given Alternative Sampling Strategies in a Climate-Adaptive Survey Design." *Frontiers in Marine Science* 10, no. July: 1–12. https://doi.org/10.3389/fmars.2023.1198260.

Bundy, A. 2001. "Fishing on Ecosystems: The Interplay of Fishing and Predation in Newfoundland Labrador." *Canadian Journal of Fisheries and Aquatic Sciences* 58, no. 6: 1153–1167. https://doi.org/10.1139/f01-063.

Chainey, S., and J. Ratcliffe. 2013. *GIS and Crime Mapping*, 448. Hoboken, New Jersey, USA: John Wiley & Sons. https://doi.org/10.1002/9781118685181.

Chambers, S. N. 2020. "The Spatiotemporal Forming of a State of Exception: Repurposing Hot-Spot Analysis to Map Bare-Life in Southern Arizona's Borderlands." *GeoJournal* 85, no. 5: 1373–1384. https://doi.org/10.1007/S10708-019-10027-Z/FIGURES/5.

Cleveland, W. S. 1993. *Visualizing Data*. Summit, NJ: Hobart Press. Internet Archive Books Collection: 360.

Crear, D. P., T. H. Curtis, S. J. Durkee, and J. K. Carlson. 2021. "Highly Migratory Species Predictive Spatial Modeling (PRiSM): An Analytical Framework for Assessing the Performance of Spatial Fisheries Management." *Marine Biology* 168, no. 10: 148. https://doi.org/10.1007/S00227-021-03951-7.

Danek, T., E. Weglinska, and M. Zareba. 2022. "The Influence of Meteorological Factors and Terrain on Air Pollution Concentration and Migration: A Geostatistical Case Study From Krakow, Poland." *Scientific Reports* 12, no. 1: 11050.

Delgado de Molina, A., L. Floch, V. Rojo, et al. 2014. "Statistics of the European and Associated Purse Seine and Baitboat Fleets, in the Atlantic Ocean." *Collective Volume of Scientific Papers ICCAT* 70, no. 6: 2654–2668.

Ding, L., K.-L. Chen, T. Liu, S.-G. Cheng, and X. Wang. 2015. "Spatial-Temporal Hotspot Pattern Analysis of Provincial Environmental Pollution Incidents and Related Regional Sustainable Management in China in the Period 1995–2012." Sustainability 7, no. 10: 14385–14407.

Dormann, C. F., M. Bobrowski, D. M. Dehling, et al. 2018. "Biotic Interactions in Species Distribution Modelling: 10 Questions to Guide Interpretation and Avoid False Conclusions." *Global Ecology and Biogeography* 27, no. 9: 1004–1016. https://doi.org/10.1111/geb.12759.

Downs, A. 2004. *Growth Management and Affordable Housing: Do They Conflict?* Washington, DC: Rowman & Littlefield. Brookings Institution Press. James A. Johnson Metro Series: 304.

Druon, J.-N., E. Chassot, L. Floch, and A. Maufroy. 2015. "Preferred Habitat of Tropical Tuna Species in the Eastern Atlantic and Western Indian Oceans: A Comparative Analysis Between FAD-Associated and Free-Swimming Schools." IOTC WPTT-17 27–16.

Druon, J. N., E. Chassot, H. Murua, and J. Lopez. 2017. "Skipjack Tuna Availability for Purse Seine Fisheries Is Driven by Suitable Feeding Habitat Dynamics in the Atlantic and Indian Oceans. Frontiers in Marine." *Science* 4, no. OCT: 298872. https://doi.org/10.3389/FMARS.2017.00315/.

Dunn, D. C., S. M. Maxwell, A. M. Boustany, and P. N. Halpin. 2016. "Dynamic Ocean Management Increases the Efficiency and Efficacy of Fisheries Management." *Proceedings of the National Academy of Sciences of the United States of America* 113, no. 3: 668–673. https://doi.org/10.1073/PNAS.1513626113/SUPPL\_FILE/PNAS.201513626SI.PDF.

Duparc, A., M. Depetris, L. Floch, P. Cauquil, P. Bach, and J. Lebranchu. 2020. "(T3) SOFTWARE A redesign for the T3 code." *Zenodo* 22: 1–5. https://doi.org/10.5281/zenodo.3878125.Changes.

Escalle, L., M. G. Pennino, D. Gaertner, et al. 2016. "Environmental Factors and Megafauna Spatio-Temporal Co-Occurrence With Purse-Seine Fisheries." *Fisheries Oceanography* 25: 433–447. https://doi.org/10.1111/fog.12163.

ESRI. 2021. How Emerging Hot Spot Analysis Works. Esri: Redlands, CA: Environmental Systems Research Institute Inc. https://pro.arc-gis.com/en/pro-app/latest/tool-reference/space-time-pattern-mining/learnmoreemerging.htm.

FAO. 2020. *The State of World Fisheries and Aquaculture 2020*. Food and Agriculture Organization of the United Nations (FAO), Fisheries and Aquaculture Department, Rome, Italy: FAO.

Fonteneau, A., D. Gaertner, A. J. Maufroy, and J. M. Amandè. 2016. "Effects of the ICCAT FAD moratorium on the tuna fisheries and tuna stocks." *Collective Volume of Scientific Papers* 72, no. 2: 520–533.

Fonteneau, A., and J. Marcille. 1993. Resources, Fishing and Biology of the Tropical Tunas of the Eastern Central Atlantic. Rome, Italy: Food and Agriculture Organization of the United Nations.

Garcia, S. M., and K. L. Cochrane. 2005. "Ecosystem Approach to Fisheries: A Review of Implementation Guidelines." *ICES Journal of Marine Science* 62, no. 3: 311–318. https://doi.org/10.1016/j.icesjms. 2004.12.003.

Getis, A., and J. K. Ord. 1992. "The Analysis of Spatial Association by Use of Distance Statistics." *Geographical Analysis* 24, no. 3: 189–206. https://doi.org/10.1111/J.1538-4632.1992.TB00261.X.

Goujon, M. 1998. "Accord des producteurs de thon congelé pour la protection des thonidés de l'Atlantique: résultats pour la flottille française." *Collective Volume of Scientific Papers ICCAT* 49, no. 3: 477–482.

Grüss, A., J. Gao, J. T. Thorson, et al. 2020. "Estimating Synchronous Changes in Condition and Density in Eastern Bering Sea Fishes." *Marine Ecology Progress Series* 635: 169–185.

Grüss, A., J. F. Walter, E. A. Babcock, et al. 2019. "Evaluation of the Impacts of Different Treatments of Spatio-Temporal Variation in Catch-Per-Unit-Effort Standardization Models." *Fisheries Research* 213, no. January: 75–93. https://doi.org/10.1016/j.fishres.2019.01.008.

Hallier, J., and D. Gaertner. 2008. "Drifting Fish Aggregation Devices Could Act as an Ecological Trap for Tropical Tuna Species." *Marine Ecology Progress Series* 353: 255–264.

Hallier, J.-P., and J. I. Parajúa. 1999. "Review of Tuna Fisheries on Floating Objects in the Indian Ocean." In *Proceedings of the International Workshop on the Ecology and Fisheries for Tunas Associated with Floating Objects. Presented at the Inter-American Tropical Tuna Commission Special Report 11, La Jolla, CA*. edited by M.D. Scott, W.H. Bayliff, C.E. Lennert-Cody, and K.M. Schaefer, 195–221. https://www.documentation.ird.fr/hor/fdi:42871.

Harley, S., and J. M. Suter. 2007. "The Potential Use of Time-Area Closures to Reduce Catches of Bigeye Tuna (*Thunnus obesus*) in the Purse-Seine Fishery of the Eastern Pacific Ocean." *Fishery Bulletin* 105: 49–61. https://spo.nmfs.noaa.gov/sites/default/files/harley.pdf.

Hazen, E. L., K. L. Scales, S. M. Maxwell, et al. 2018. "A Dynamic Ocean Management Tool to Reduce Bycatch and Support Sustainable Fisheries." *Science Advances* 4, no. 5: eaar3001. https://doi.org/10.1126/SCIADV.AAR3001.

Hilborn, R., K. Stokes, J. J. Maguire, et al. 2004. "When Can Marine Reserves Improve Fisheries Management?" *Ocean and Coastal Management* 47, no. 3–4: 197–205. https://doi.org/10.1016/j.ocecoaman. 2004.04.001.

Hobday, A. J., J. R. Hartog, T. Timmiss, and J. Fielding. 2010. "Dynamic Spatial Zoning to Manage Southern Bluefin Tuna (*Thunnus maccoyii*) Capture in a Multi-Species Longline Fishery." *Fisheries Oceanography* 19, no. 3: 243–253. https://doi.org/10.1111/J.1365-2419.2010.00540.X.

Hobday, A. J., S. M. Maxwell, J. Forgie, et al. 2014. "Dynamic Ocean Management: Integrating Scientific and Technological Capacity With Law, Policy, and Management." *Stanford Environmental Law Journal* 33, no. 2: 125–165.

ICCAT. 2019. Report of the 2019 ICCAT Yellowfin Tuna Stock Assessment Meeting. Madrid, Spain: Collective Volume of Scientific Papers.

ICCAT. 2021. "Report of the 2021 Bigeye Tuna Data Preparatory Meeting." 78(2), 46–143.

ICCAT. 2022. "Report of the 2022 Skipjack Stock Assessment Meeting." 79, 87.

ISSF. 2024. Status of the World Fisheries for Tuna. March 2024 ISSF Technical Report 2024–02. Pittsburgh, PA: International Seafood Sustainability Foundation.

Jimenez, R., and P. Wongchanapai. 2022. "A Decade Review of Disease Surveillance Research Trends in the International Journal of Health Geographics (2009 to 2018)."

Kaplan, D. M., E. Chassot, J. M. Amandé, et al. 2014. "Spatial Management of Indian Ocean Tropical Tuna Fisheries: Potential and Perspectives." *ICES Journal of Marine Science* 71, no. 7: 1728–1749. https://doi.org/10.1093/ICESJMS/FST233.

Kass, R. E., and D. Steffey. 1989. "Approximate Bayesian Inference in Conditionally Independent Hierarchical Models (Parametric Empirical Bayes Models)." *Journal of the American Statistical Association* 84, no. 407: 717–726.

Kitakado, T., S. Wang, K. Satoh, et al. 2021. "Updated report of trilateral collaborative study among Japan, Korea and Taiwan for producing joint abundance indices for the yellowfin tunas in the Indian Ocean using longline fisheries data up to 2020." IOTC-2021-WPTT23-11.

Lopez, J., G. Moreno, C. Lennert-Cody, et al. 2017. "Environmental Preferences of Tuna and Non-Tuna Species Associated With Drifting Fish Aggregating Devices (DFADs) in the Atlantic Ocean, Ascertained Through Fishers' Echo-Sounder Buoys." *Deep-Sea Research Part II: Topical Studies in Oceanography* 140: 127–138. https://doi.org/10.1016/J.DSR2.2017.02.007.

Mann, H. B. 1945. "Nonparametric Tests Against Trend." *Econometrica* 13, no. 3: 245. https://doi.org/10.2307/1907187.

Maxwell, S. M., E. L. Hazen, R. L. Lewison, et al. 2015. "Dynamic Ocean Management: Defining and Conceptualizing Real-Time Management of the Ocean." *Marine Policy* 58: 42–50. https://doi.org/10.1016/J. MARPOL.2015.03.014.

Miyake, M. P., P. Guillotreau, C.-H. Sun, and G. Ishimura. 2010. Recent developments in the tuna industry: stocks, fisheries, management, processing, trade and markets. Rome, Italy: FAO.

Mondal, S. 2020. "Modeling the Spatial Pattern of Household Quality of Living in West Bengal: An Approach of Hotspot and Cluster Analysis." *Modeling Earth Systems and Environment* 6, no. 2: 833–851.

Monnahan, C. C., J. T. Thorson, S. Kotwicki, N. Lauffenburger, J. N. Ianelli, and A. E. Punt. 2021. "Incorporating Vertical Distribution in Index Standardization Accounts for Spatiotemporal Availability to Acoustic and Bottom Trawl Gear for Semi-Pelagic Species." *ICES Journal of Marine Science* 78, no. 5: 1826–1839. https://doi.org/10.1093/ICESJMS/FSAB085.

Ord, J. K., and A. Getis. 1995. "Local Spatial Autocorrelation Statistics: Distributional Issues and an Application." *Geographical Analysis* 27, no. 4: 286–306. https://doi.org/10.1111/J.1538-4632.1995.TB00912.X/ABSTRACT.

Pallarés, P., and J. P. Hallier. 1997. "Analyse du schéma d'échantillonnage multispécifique des thonidés tropicaux." *Rapport Scientifique. IEO/ORSTOM, Programme* 95: 37.

Pascual-Alayón, P., L. Floch, F. N'gom, et al. 2019. "Statistics of the European and Associated Purse Seine and Baitboat Fleets, in the Atlantic Ocean (1991-2017)." *ICCAT Recueil de Documents Scientifiques/Collective Volume of Scientific Paper* 75, no. 7: 1992–2006.

Pérez, G., L. Dagorn, J.-L. Deneubourg, et al. 2020. "Effects of Habitat Modifications on the Movement Behavior of Animals: The Case Study of Fish Aggregating Devices (FADs) and Tropical Tunas." *Movement Ecology* 8, no. 1: 47. https://doi.org/10.1186/s40462-020-00230-w.

Perez, I., L. Guéry, M. Authier, and D. Gaertner. 2022. "Assessing the Effectiveness of dFADs Fishing Moratorium in the Eastern Atlantic Ocean for Conservation of Juvenile Tunas From AOTTP Data." Fisheries Research 253: 106360. https://doi.org/10.1016/J.FISHRES.2022.106360.

Pinto, C., M. Travers-Trolet, J. I. Macdonald, E. Rivot, and Y. Vermard. 2019. "Combining Multiple Data Sets to Unravel the Spatiotemporal Dynamics of a Data-Limited Fish Stock." *Canadian Journal of Fisheries and Aquatic Sciences* 76, no. 8: 1338–1349. https://doi.org/10.1139/cjfas -2018-0149.

Planet Tuna. 2020. "Atlantic Bluefin Tuna: The Path to an Amazing Recovery." https://planettuna.com/en/atlantic-bluefin-tuna-the-path-to-an-amazing-recovery/.

R Core Team. 2021. R: A Language and Environment for Statistical Computing. Vienna, Austria: R Foundation for Statistical Computing. https://www.r-project.org/.

Rahman, M. R., A. H. M. H. Islam, and M. N. Islam. 2021. "Geospatial Modelling on the Spread and Dynamics of 154 Day Outbreak of the Novel Coronavirus (COVID-19) Pandemic in Bangladesh Towards

Vulnerability Zoning and Management Approaches." *Modeling Earth Systems and Environment* 7, no. 3: 2059–2087.

Rogers, A., G. Galland, A. Nickson, G. Macfadyen, T. I. M. Huntington, and V. Defaux. 2016. *Netting Billions: A Global Valuation of Tuna*. Corvalis, OR: Oregon State University.

Rose, G. A., and R. L. O'Driscoll. 2002. "Capelin Are Good for Cod: Can the Northern Stock Rebuild Without Them?" *Journal of Materials Science* 59: 1018–1026.

Satoh, K., H. Xu, C. V. Minte-Vera, M. N. Maunder, and T. Kitakado. 2021. "Size-Specific Spatiotemporal Dynamics of Bigeye Tuna (*Thunnus obesus*) Caught by the Longline Fishery in the Eastern Pacific Ocean." *Fisheries Research* 243, no. July: 106065. https://doi.org/10.1016/j.fishres.2021.106065.

Schirripa, M. J. 2016. "An Assessment of Atlantic Bigeye Tuna for 2015." *Collective Volume of Scientific Papers ICCAT* 72, no. 2: 428–471.

Sibert, J., I. Senina, P. Lehodey, and J. Hampton. 2012. "Shifting From Marine Reserves to Maritime Zoning for Conservation of Pacific Bigeye Tuna (*Thunnus obesus*)." *Proceedings of the National Academy of Sciences of the United States of America* 109, no. 44: 18221–18225. https://doi.org/10.1073/PNAS.1209468109/ASSET/9171937F-23AD-4C13-BC24-38C79 CC4CF80/ASSETS/GRAPHIC/PNAS.1209468109FIG04.JPEG.

Stephan, P., D. Gaertner, I. Perez, and L. Guéry. 2022. "Multi-Species Hotspots Detection Using Self-Organizing Maps: Simulation and Application to Purse Seine Tuna Fisheries Management." *Methods in Ecology and Evolution* 00: 2850–2864. https://doi.org/10.1111/2041-210X. 14008.

Thorson, J. T. 2019. "Guidance for Decisions Using the Vector Autoregressive Spatio-Temporal (VAST) Package in Stock, Ecosystem, Habitat and Climate Assessments." *Fisheries Research* 210, no. February: 143–161. https://doi.org/10.1016/j.fishres.2018.10.013.

Thorson, J. T., C. F. Adams, E. N. Brooks, et al. 2020. "Seasonal and Interannual Variation in Spatio-Temporal Models for Index Standardization and Phenology Studies." *ICES Journal of Marine Science* 77, no. 5: 1879–1892. https://doi.org/10.1093/ICESJMS/FSAA074.

Torres-Irineo, E., D. Gaertner, A. D. De Molina, and J. Ariz. 2011. "Effects of Time-Area Closure on Tropical Tuna Purse-Seine Fleet Dynamics Through Some Fishery Indicators." *Aquatic Living Resources* 24, no. 4: 337–350. https://doi.org/10.1051/ALR/2011143.

Vasilakopoulos, P., F. G. Oneill, and C. T. Marshall. 2011. "Misspent Youth: Does Catching Immature Fish Affect Fisheries Sustainability?" *ICES Journal of Marine Science* 68, no. 7: 1525–1534. https://doi.org/10.1093/icesjms/fsr075.

Vasilakopoulos, P., F. G. O'Neill, and C. T. Marshall. 2012. "Differential Impacts of Exploitation Rate and Juvenile Exploitation on NE Atlantic Fish Stock Dynamics Over the Past Half Century." *Fisheries Research* 134–136: 21–28. https://doi.org/10.1016/j.fishres.2012.08.006.

Vidal, T. 2020. "Developing Yellowfin Tuna Recruitment Indices From Drifting FAD Purse Seine Catch and Effort Data." WCPFC-SC16-2020/SA-IP-08.

Vidal, T., P. Hamer, L. Escalle, and G. Pilling. 2020. "Assessing Trends in Skipjack Tuna Abundance From Purse Seine Catch and Effort Data in the WCPO." WCPFC-SC16-2020/SA-IP-09.

Xu, H., C. E. Lennert-Cody, M. N. Maunder, and C. V. Minte-Vera. 2019. "Spatiotemporal Dynamics of the Dolphin-Associated Purse-Seine Fishery for Yellowfin Tuna (*Thunnus albacares*) in the Eastern Pacific Ocean." *Fisheries Research* 213, no. September 2018: 121–131. https://doi.org/10.1016/j.fishres.2019.01.013.

#### **Supporting Information**

Additional supporting information can be found online in the Supporting Information section.